European Journal of Neuroscience, Vol. 12, pp. 767–770, 2000

SHORT COMMUNICATION
Does the migraine aura reflect cortical organization?

M. A. Dahlem[1,2], R. Engelmann[2], S. Löwel[2] and S. C. Müller[1]
[1]Otto-von-Guericke-Universität Magdeburg, Institut für Experimentelle Physik, Abteilung Biophysik, Universitätsplatz 2, D-39016 Magdeburg, Germany
[2]Leibniz-Institut für Neurobiologie (IfN), Zentrum für Lern- und Gedächtnisforschung, Forschergruppe: Visuelle Entwicklung und Plastizität, Brenneckestraße 6, D-39118 Magdeburg, Germany

Keywords: cat, hallucination, orientation selectivity, primary visual cortex, spreading depression

Abstract

Individuals suffering from classical migraine report an astonishing diversity of migraine auras. A frequently reported symptom is a visual hallucination known as fortification illusion (FI). Here we demonstrate that the typical zig-zag pattern of the FI can be reproduced using experimental data of orientation maps of the primary visual cortex (V1) assuming that a continuous excitation front propagates across V1. We put forward a model in which the cortical neurons within this excitation wave are activated sufficiently to contribute to conscious perception. It is shown that the discontinuous repetitive nature of the zig-zag pattern of the FI can reflect the specific layout of visual cortical orientation maps. Additionally, dynamic features of the FI are predicted based on our model.

A plethora of hallucinations is reported by patients suffering from classical migraine, the so-called migraine auras (Wilkinson & Robinson, 1985; Sacks, 1992; Queiroz *et al.*, 1997; Shibata *et al.*, 1998). Individuals report primarily visual or tactile auras, but other sensory phenomena have been experienced, too. However, this sensory characterization may not reflect differences in the underlying neuronal disorder, but rather the functional differentiation of the neocortex. A frequently occurring visual symptom of the migraine aura is known as fortification illusion (FI) or zig-zag pattern. Figure 1 shows a repeatedly reproduced picture of the FI drawn by the psychologist Karl Lashley (1941); the patterns of lines and angles are much the same in the experience of all persons who have reported them.

The characteristic form and development of the FI suggests that the underlying phenomenon is a wave propagating through the primary visual cortex (Lashley, 1941), possibly the cortical spreading depression (CSD) (Milner, 1958; Lauritzen, 1994; Welch, 1997). Assuming a wave with a constant propagation speed in the visual cortex, the eccentricity of the FI in the contralateral visual hemifield is well described by the distribution of the retino-cortical magnification factor (Grüsser, 1995). The demonstration of unique changes of cerebral blood flow during attacks of migraine with aura have been replicated in animal experiments during CSD and thus constitute another important line of support for the spreading depression theory, as reviewed by Lauritzen (1994). However, the CSD theory of migraine is critically discussed (Lauritzen, 1994; Olsen, 1995), and a peculiar feature of the aura, namely the shape of the zig-zag pattern, remains a mystery.

Correspondence: Markus Dahlem, at [1]Otto-von-Guericke-Universität Magdeburg, as above.
E-mail: dahlem@physik.uni-magdeburg.de

Received 9 July 1999, revised 26 November 1999, accepted 15 December 1999

Richards (1971) proposed a hexagonal arrangment of cortical neurons to explain the origin of the FI pattern, based on his assumption that radial lines perpendicular to the curved FI front are nearly absent. In a more elaborated model an interaction of a traveling wave with individual hypercolumns based on lateral inhibition was suggested (Schwartz, 1980), without considering a specific layout of the iso-orientation domains (see below). More recently, Reggia & Montgomery (1996) created a reaction-diffusion model for CSD coupled to a one-layer lateral inhibitory neural network to explain the FI. Their simulated cortical excitation pattern displayed irregular patches and lines which were projected onto the visual field. As shown earlier (Ermentrout & Cowan, 1979), the topographic mapping from cortex to retina can transform simple global geometric excitation patterns in the cortex into 'form constants' seen during drug-induced visual hallucinations (Klüver, 1967), but local repetitive patterns ('mosaics') remain virtually unchanged under the retinotopic transformation, except for distortions. Accordingly, the retinotopic map cannot account for the local zig-zag pattern, but it determines the entire kidney-like shape (see Fig. 1) of the visual disturbance. Here, we propose that the perceived migraine halluzinations are generated by a planar excitation wave (CSD-like event) propagating across the primary visual cortex (V1), and that the peculiar zig-zag front of the FI reflects the cortical organization of orientation preference.

In general, the response properties of neurons in V1 to visual information are exceedingly well organized, albeit complex. First, V1 is retinotopically organized such that stimulating neighbouring points in the visual field leads to activation of neighbouring neurons in the cortex. Another major functional property of visual cortical neurons is their orientation selectivity, i.e. the fact that the cells fire maximally when a contour of a particular orientation appears within their receptive field. As demonstrated by single-unit recording (Hubel & Wiesel, 1962) and, more recently, with optical imaging techniques (Blasdel & Salama, 1986; Grinvald *et al.*, 1986; Ts'o *et al.*, 1990), neurons with similar prefrerred orientations are clustered together and

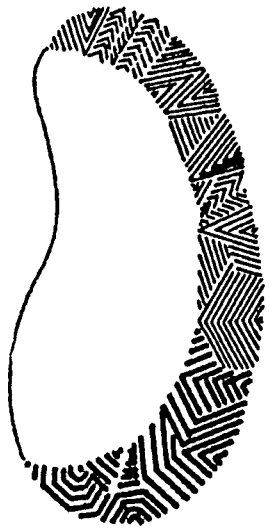

FIG. 1. Sketch of the fortification illusion drawn by Karl Lashley (1941). The kidney-shaped visual disturbance exhibits a typical zig-zag pattern at its convex side, while the inner part corresponds to a scotoma (blind area). Usually the disturbance starts close to the fovea and increases in size as it accelerates to the periphery (from Lashley, 1941; copyright 1941, American Medical Association).

not distributed randomly across the cortical surface. The layout of orientation preference in the visual cortex is characterized by iso-orientation domains that are arranged around centres in a pinwheel-like fashion (Blasdel & Salama, 1986; Bonhoeffer & Grinvald, 1991).

Both the retinotopic and the orientation map are features of the primary visual cortex which we have used to simulate the shape of the zig-zag pattern. Using optical imaging of intrinsic signals, activity maps in V1 (area 17) of cats were recorded in regions of 4.8×3.6 mm at the junction of the lateral to the posterolateral gyrus of the brain. Animals were stimulated with moving gratings of four different orientations [0, 45, 90 and 135°; spatial frequency 0.5 cyc/deg; speed 4 °/s; the methodology is described in detail by Löwel *et al.* (1998), see also Bonhoeffer & Grinvald (1996) for further details]. For comprehensive analysis, the single responses to all different stimulus conditions were summed vectorially for every point in the cortex. In the resulting orientation preference map ('angle map'; Blasdel & Salama, 1986; Bonhoeffer & Grinvald, 1991), illustrated in Fig. 2A, the preferred orientation for every point is indicated in a grey-scale code. Orientation (pinwheel) centres were detected using a semiautomatic method. The average pinwheel distance (APD) was defined as the square root of the reciprocal area density of pinwheels.

The APD of the visual cortex illustrated in Fig. 2A was 571 μm. In the diagram in Fig. 2B, a profile of the observed orientation angles along the horizontal line in the middle of Fig. 2A was plotted. At the top of Fig. 2B, the profile is shown in grey-scale code. The profile was divided into equal fragments with lengths of 575 μm. This value is closest to the APD whilst being an integral multiple of the maximum spatial resolution for the image (25 μm/pixel). For each of the seven resulting fragments an average orientation vector $\vec{v}$ was calculated, and represented by a bar that was rotated such that its orientation was parallel to the direction of vector $\vec{v}$. Computations use pixel-wise summing for $k=1$ to N, to produce the vector $\vec{v}=\{\sum_k^N \exp(i\Theta_k)\}/N$, where the phase Θ_k is given by $\Theta_k=2\varphi_k$, and φ_k is the preferred orientation angle at pixel position k. The average angle is then $\varphi_{ave}=\arg(\vec{v})/2$. Formally, this method is equal to vector methods used to estimate population codes (Georgopoulos *et al.*, 1986; Seung & Sompolinsky, 1993), but in our case is applied to optical imaging data. As can be seen the vector $\vec{v}$ is normalized. If the orientation preferences of the pixels over which the average is taken are similar, then the value of l will be close to 1; if the preferences vary widely then l will be close to 0. The vector magnitude l can thus be regarded as a measure of dominance among the fragments. Therefore the vector magnitude l can be taken as a measure of how dominant the calculated average angle is in the calculated field.

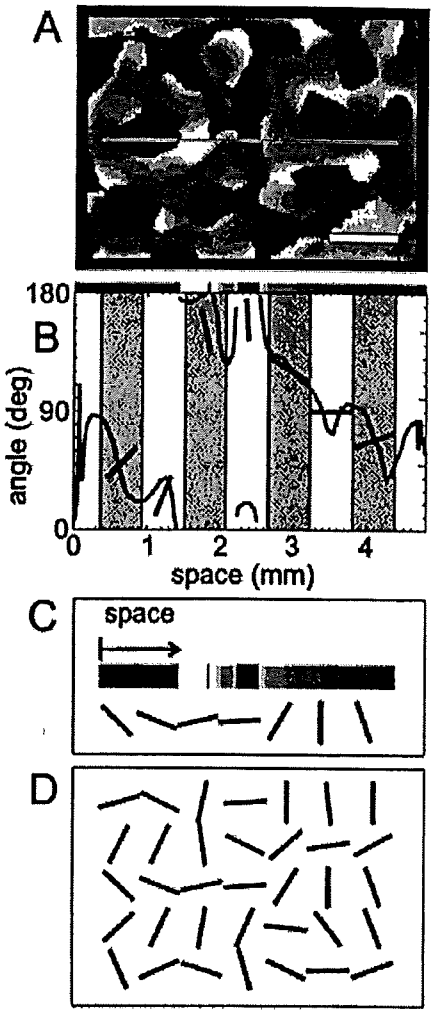

FIG. 2. (A) Optically visualized orientation columns in V1 (area 17) of the cat. Scale bar (bottom right), 1 mm. (B) The spatial distribution of orientation angles (0–180°) along the horizontal centre line of image in A. At the top of the diagram these orientation angles are shown in a grey-scale code. Seven sections of equal length (575 μm ≈ average pinwheel distance) are alternately highlighted in grey and white: in each section, a bar is plotted at the orientation of the vectorially averaged corresponding angle data. (C, upper) Orientation angles (from B) shown in grey-scale code and (C, lower) represented by seven bars. (D) Thirty-five bars are plotted, in the same way as in the lower part of C, at a horizontal and vertical distance of 575 μm from each other. The change in orientation between adjacent bars represents the underlying symmetry of the orientation map.

The resulting sequence of bars is shown in Fig. 2C. If these bars represent an illusive stimulation within the visual field, one has to take into account the retino-cortical magnification factor. However, since the retinotopic mapping can be described by a complex logarithmic function which implies that angles are preserved and that

FIG. 3. Simulation of the fortification illusion. Multiple bars with white margins were plotted in the order of their dominance. The pattern resembles a snapshot of a fraction of the moving zig-zag front.

the magnification factor is locally isotropic (Schwartz, 1977), and since we consider only the local features of the FI pattern, a back transformation to the visual field does not require an exponential function. To show the distribution of the bars in a larger area, four additional lines, which were parallel to the middle line in Fig. 2A and symmetrically placed at a distance of 575 μm and 1150 μm so that the rotated bars do not intersect, were equally fragmented and rotated as described above (Fig. 2D). The resulting pattern comprises the basic symmetry of the orientation map and is reminiscent of a fortification illusion.

Given a CSD wave with a velocity of ~ 50 μm/s that generates during 10 s (see below) a sufficiently strong signal to stimulate cortical neurons, the effective width of the excited cortical area is ~500 μm. Within this area Γ of 500 μm width we assume that the neurons are excited to contribute to hallucinatory perception. The average vector $\vec{v}$ was calculated for line fragments γ (25 × 575 μm) in each case parallel to the assumed excitation front, because these neurons are activated synchronously. This calculation was repeated in increments of 50 μm, starting in the upper left corner of area Γ until the entire area was covered. In this way, a total of 869 vectors $\vec{v}$ (79 fragments in 11 lines) was calculated, each having its particular orientation and a certain magnitude *l*, which was normalized to values between 0 and 1, representing its dominance. Again, the orientations were plotted as bars, each at its spatial location (Fig. 3). Since the bars now possibly intersect, they were plotted in the order of their dominance on top of each other as white-black-white steps, representing the basic structure of the receptive field of simple cells in V1. Hereby, the size of the black surface of a single bar matches the size of the fragment γ, and both white margins have half the width of the fragment. Alternatively, the aspect ratio of the bars could be changed, thereby changing the density of the resulting stripes in Fig. 3. However, migraine patients reported that the distinct lines cannot be counted, because the whole pattern of the FI appears to oscillate at 10 Hz, but they have the impression of groups of five or more parallel lines (Lashley, 1941). This impression might be related to the structure of the receptive field of complex cells in V1, but this is beyond the scope of this model. Consequently, the width of the bars is not critical for a comparison of our simulated FI with those observed empirically.

The resulting pattern illustrated in Fig. 3 displays features of the fortification illusion: distinct domains of roughly parallel lines are present, each domain having a specific angle with respect to the adjacent domain. Our simulations lead us to predict that the zig-zag pattern perceived by individuals suffering from classical migraine reflects the local organization of their visual cortical orientation map. Domains of bars with similar orientation in the simulated zig-zag pattern change their orientation by ~ 90°, as one crosses over a pinwheel singularity to the opposite side. Furthermore, fractures, i.e. areas where the change of orientation preference is most pronounced (Blasdel & Salama, 1986), are located at the borders of two distinct groups of roughly parallel lines. It was proposed that the retinotopic mapping is distorted near such orientation fractures (Durbin & Mitchison, 1990), which could be explored by analysis of the fortification illusion of migraine patients. Saddle points and linear zones (Swindale, 1996) are not yet clearly seen in the simulation.

A particularly interesting point for future analysis of the visual hallucinations is to characterize the dynamic properties of the 'kaleidoscopic change', as it was called by Karl Lashley (1941), while the FI is propagating through the visual field. According to our explanation of the origin of the FI, some bars should change their orientation clockwise for a certain period of time, while others should rotate counterclockwise. To visualize the dynamics of our simulated FI, we created an MPEG movie (http://iep463.nat.uni-magdeburg.de/dahlem/dynamic_fi.html) by calculating single images of the aura as seen in Fig. 3 for subsequent wave locations. In this movie there are, in fact, several transitions from one direction of rotation to the other. If these transitions are observed by migraine sufferers, the average time between two transitions should be approximately the reciprocal CSD velocity multiplied by the APD in man (12 s ~ 1/(50 μm/s) × 592 μm). The APD in man can be estimated to be ~ 592 μm by extrapolating to humans the relationship between cytochrome oxidase blob density and pinwheel density as observed in monkeys. In macaque monkeys, one finds roughly two pinwheels per blob (but their centres do not coincide; Bartfeld & Grinvald, 1992). In human visual cortex, the density of cytochrome oxidase blobs was reported to be one blob per 0.6–0.8 mm^2 (Horton & Hedley-Whyte, 1984); the APD in man is then $\sqrt{\{0.7\,mm^2/2\}} \simeq 592\ \mu m^2$.

The spatial distance of counter-rotating bars in the visual field depends on the local magnification factor. Our simulations show that this distance is in the order of the APD, and close to the value we assumed for the width of Γ. Therefore, in the visual field the spatial distance of counter-rotating bars can be predicted to be close to the width of the FI.

The pattern in Fig. 3 is created by using the angular data (orientation information) of a certain area and transforming them back to a representation by bars of the calculated average orientation. In this procedure, the only information required in addition to the measured orientation angles is the width of the area Γ, and the width and length of its subdivisions γ. An important question is how the width of the stimulating CSD wave is defined, which in turn determines the width of area Γ and the width of the simulated zig-zag

front. First, we consider the problem of how a CSD wave (or a CSD-like event) can possibly produce a signal accessible to perception? CSD is characterized by a transient high-amplitude signal in all major ions that develops into an intercellular wave coordinating the cellular responses within the grey matter. At the plateau of the CSD attack, the affected neurons are in a state which makes their participation in signal processing highly unlikely. Therefore this phase presumably corresponds to the scotoma in the back of the zig-zag front and the zig-zag front itself could correspond to the onset of CSD. During the onset, single-unit activity recording shows intense high-frequency impulse bursts that last for a few seconds (Lauritzen, 1994). The following steep rise of nearly all signals observed during CSD occurs within < 15 s. In the illustrated simulation, we assume a value of 10 s for the duration of excitation.

To realize a discrete subdivision over which the average orientation was calculated vectorially we introduced an additional parameter γ. Its value was chosen to be a characteristic length scale of the map, because the APD can be expected to scale with the average spacing of the iso-orientation domains (Swindale, 1992). We should note that the periodicity of these domains is considered to be a factor of $\sim \sqrt{\{\pi\}}$ larger than the APD (Wolf & Geisel, 1998). If too large a value of this parameter is chosen (over twice the APD), the average orientation of a cortical area of that length no longer provides a significant value, because all orientations are almost equally distributed in that area. If the parameter value chosen is too small, the resulting pattern corresponds to a field orientation plot of the orientation map ignoring the modular structure of V1. Finally, there is the related problem of how to choose the width of the line fragment γ. In Fig. 3, the chosen width was considerably smaller than the APD, although the overall pattern resulting from our simulation is fairly robust against realistic changes in the size of the surface of γ. It remains to be seen in future investigations whether single features are more pronounced by changing the size of γ.

In summary, we suggest that one frequently reported visual symptom of the migraine aura, namely the FI, can be reproduced by assuming that a continuous and smooth CSD-like excitation front propagates across the primary visual cortex. We present evidence that its typical zig-zag pattern reflects features of the organization of orientation preference maps in V1. It should be noted that the previous models developed from similar ideas as presented here (Richards, 1971) were followed by models introducing heterogeneous action via lateral inhibition (Schwartz, 1980) and models of disrupted wavefronts disregarding orientation selectivity (Reggia & Montgomery, 1996). Our approach predicts dynamic features of the FI such as counter-rotating bars, which are not yet sufficiently well documented. If these features are found in man, the zig-zag pattern and analogue aura hallucinations may indeed be a reflection of cortical organization. If this is so, the aura would provide a particularly rich domain that may yield important insights into the functional organization of the human visual system.

Acknowledgements

We thank B. Hassenstein for initiating a discussion about the reported topic, F. Wolf for computational work on the optical imaging data and J. M. Crook, U. Storb and L. van Hemmen for helpful discussions. This work was partially supported by the Deutsche Forschungsgemeinschaft.

Abbreviations

APD, average pinwheel distance; CSD, cortical spreading depression; FI, fortification illusion; V1, primary visual cortex.

References

Bartfeld, E. & Grinvald, A. (1992) Relationships between orientation-preference pinwheels, cytochrome oxidase blobs, and ocular-dominance columns in primate striate cortex. *Proc. Natl Acad. Sci. USA*, **89**, 11905–11909.

Blasdel, G.G. & Salama, G. (1986) Voltage-sensitive dyes reveal a modular organization in monkey striate cortex. *Nature*, **321**, 579–585.

Bonhoeffer, T. & Grinvald, A. (1991) Iso-orientation domains in cat visual cortex are arranged in pinwheel-like patterns. *Nature*, **353**, 429–431.

Bonhoeffer, T. & Grinvald, A. (1996) Optical Imaging based on Intrinsic Signals: The Methodology. In Toga, A. & Mazziotta, J.C. (eds), *Brain Mapping: the Methods*. Academic Press, San Diego, pp. 55–97.

Durbin, R. & Mitchison, G. (1990) A dimension reduction framework for understanding cortical maps. *Nature*, **343**, 644–647.

Ermentrout, G.B. & Cowan, J.D. (1979) A mathematical theory of visual hallucination patterns. *Biol. Cybern.*, **34**, 137–150.

Georgopoulos, A.P., Schwartz, A.B. & Kettner, R.E. (1986) Neuronal population coding of movement direction. *Science*, **233**, 1416–1419.

Grinvald, A., Lieke, E., Frostig, R.D., Gilbert, C.D. & Wiesel, T.N. (1986) Functional architecture of cortex revealed by optical imaging of intrinsic signals. *Nature*, **324**, 361–364.

Grüsser, O.-J. (1995) Migraine phosphenes and the retino-cortical magnification factor. *Vision Res.*, **35**, 1125–1134.

Horton, J.C. & Hedley-Whyte, E.T. (1984) Mapping of cytochrome oxidase patches and ocular dominace columns in human visual cortex. *Phil. Trans. R Lond. B Biol. Sci.*, **304**, 255–272.

Hubel, D.H. & Wiesel, T.N. (1962) Receptive fields, binocular interaction and functional architecture in the cat's visual cortex. *J. Physiol. (Lond.)*, **160**, 106–154.

Klüver, H. (1967). *Mescal and the Mechanism of Hallucinations*. University Press of Chicago, Chicago.

Lashley, K. (1941) Patterns of Cerebral Integration Indicated by the Scotoma of Migraine. *Arch. Neurol. Psychiatry*, **46**, 331–339.

Lauritzen, M. (1994) Pathophysiology of the migraine aura. The spreading depression theory. *Brain*, **117**, 199–210.

Löwel, S., Schmidt, K.E., Dae-Shik, K., Wolf, F., Hoffsümmer, F., Singer, W. & Bonhoeffer, T. (1998) The layout of orientation and ocular dominace domains in area 17 of strabismic cats. *Eur. J. Neurosci.*, **10**, 2629–2643.

Milner, P.M. (1958) Note on a possible correspondence between the scotoma of migraine and the spreading depression of Leão. *Electroencephalogr. Clin. Neurophysiol.*, **10**, 705–706.

Olsen, T.S. (1995) Pathophysiology of the migraine aura: the spreading depression theory. *Brain*, **118**, 307–308.

Queiroz, L.P., Rapoport, A.M., Weeks, R.E., Sheftell, F.D., Siegel, S.E. & Baskin, S.M. (1997) Characteristics of migraine visual aura. *Headache*, **37**, 137–141.

Reggia, J.A. & Montgomery, D. (1996) A computational model of visual hallucinations in migraine. *Comput. Biol. Med.*, **26**, 133–141.

Richards, W. (1971) The fortification illusion of migraines. *Sci. Am.*, **224**, 88–96.

Sacks, O. (1992) *Migraine*, 2nd edn, University of California Press, Berkley, pp. 51–98.

Schwartz, E. (1977) Spatial mapping in the primate sensory projection: analyticstructure and relevance to perception. *Biol. Cybern.*, **25**, 181–194.

Schwartz, E. (1980) A quantitative model of the functional architecture of human striate cortex with application to visual illusion and cortical texture analysis. *Biol. Cybern.*, **37**, 63–76.

Seung, H.S. & Sompolinsky, H. (1993) Simple models for reading neuronal population codes. *Proc. Natl Acad. Sci. USA*, **90**, 10749–10753.

Shibata, K., Osawaand, M. & Iwata, M. (1998) Pattern reversal visual evoked potentials in migraine with aura and migraine aura without headache. *Cephalalgia*, **18**, 319–323.

Swindale, N.V. (1992) A model for the coordinated development of columnar systems in primate striate cortex. *Biol. Cybern.*, **66**, 217–230.

Swindale, N.V. (1996) The development of topography in the visual cortex: a review of models. *Network: Computation Neural Systems*, **7**, 161–247.

Ts'o, D.Y., Frostig, R.D., Lieke, E,E. & Grinvald, A. (1990) Functional organization of primate visual cortex revealed by high resolution optical imaging. *Science*, **249**, 417–420.

Welch, K.M. (1997) Pathogenesis of migraine. *Semin. Neurol.*, **17**, 335–341.

Wilkinson, M. & Robinson, D. (1985) Migraine art. *Cephalalgia*, **5**, 151.

Wolf, F. & Geisel, T. (1998) Spontaneous pinwheel annihilation during visual development. *Nature*, **395**, 73–78.